A chromatinized origin reduces ORC mobility and spatially constrains MCM

Author list:

Humberto Sánchez[1], Zhaowei Liu[1], Edo van Veen[1], Theo van Laar[1], Belén Solano[1], John F. X. Diffley[2], and Nynke H. Dekker[1]

Affiliations:

[1]Department of Bionanoscience, Kavli Institute of Nanoscience, Delft University of Technology, Delft, The Netherlands.
[2] Chromosome Replication Laboratory, Francis Crick Institute, London, UK.

ABSTRACT

Chromatin replication involves the assembly and activity of the replisome within the nucleosomal landscape. At the core of the replisome is the Mcm2-7 complex (MCM), which is loaded onto DNA after binding to the Origin Recognition Complex (ORC). In yeast, ORC is a dynamic protein that diffuses rapidly along DNA, unless halted by origin recognition sequences. However, less is known about the dynamics of ORC proteins in the presence of nucleosomes and attendant consequences for MCM loading. To address this, we harnessed an *in vitro* single-molecule approach to interrogate a chromatinized origin of replication. We find that ORC binds the origin of replication with similar efficiency independently of whether the origin is chromatinized, despite ORC mobility being reduced by the presence of nucleosomes. Recruitment of MCM also proceeds efficiently on a chromatinized origin, but subsequent movement of MCM away from the origin is severely constrained. These findings suggest that chromatinized origins in yeast are essential for the local retention of MCM, which may enhance the ease of replisome assembly.

KEYWORDS

DNA replication, yeast replication, replication origin, chromatin, nucleosomes, ORC, Mcm2-7/Cdt1, MCM, target search, protein diffusion

INTRODUCTION

Eukaryotic genomes are structurally organized as a combination of DNA and proteins known as chromatin. Cell biology, genetics, and biochemical experiments have demonstrated that the quantity and local density of the basic structural unit of chromatin, the nucleosome, can define where the initiation of DNA replication happens and that chromatin folding influences replication timing[1]. Less is known about the influence of nucleosomes on the individual proteins that are involved in establishing DNA replication, and their attendant dynamics.

DNA replication in eukaryotes occurs during the S phase of the cell cycle, during which the entire genome must be duplicated in a coordinated manner. In the budding yeast *Saccharomyces cerevisiae*, replication is initiated from hundreds of sequence-specific origins of replication. Each origin is prepared for replication initiation in two temporally separated steps that are essential for proper DNA replication[2]. During the G1 phase of the cell cycle, the Origin Recognition Complex (ORC) first binds to replication origins[3]. These origins are autonomous replicating sequences (ARS) that contain both a strong binding site (the ARS consensus sequence, or ACS) and a weak binding site (B2) for ORC. Once bound, ORC, together with Cdc6 and Cdt1, then loads two inactive Mcm2-7 (MCM) replicative DNA helicases, forming the pre-replication complex (pre-RC); this is known as the licensing step[4, 5]. During S phase, origins of replication are activated by the combined action of two kinases, S-CDK and DDK, which bring Cdc45 and GINS into association with MCM to form the active replicative helicase CMG complex, in the step known as firing[6-8]. The addition of DNA polymerases and other replisome-associated proteins completes the assembly of the full replisome and allows DNA replication to proceed[8, 9].

During the licensing step ORC, Cdc6 and MCM/Cdt1 are bound to DNA replication origins that are embedded in the chromatin[2]. Biochemical studies have shown that origins are free of nucleosomes[10], and genome-wide analysis suggests that the existence of such nucleosome-free regions (NFRs) at origins favors ORC binding[11]. Conversely, ORC has an active role in the positioning of nucleosomes around the origin[12]. Origin licensing is also influenced by chromatin remodeling enzymes that act at the origin[13], and recently a novel role for ORC in the coordination of chromatin remodeler activity before and during replication has been established[14].

We have previously demonstrated that yeast ORC is a mobile protein that rapidly diffuses on bare DNA, but that origin recognition halts this search process[15]. Furthermore, it has been observed that MCM diffuses on DNA[4, 5] and that nucleosomes can act as potential obstacles for MCM diffusion[16], so we sought to investigate the roles of origin-flanking nucleosomes in either directly limiting or locally targeting the diffusion of ORC and, consequently, in the loading of MCM onto the DNA.

RESULTS

Establishment of a labeled chromatinized origin of replication within 10.4 kbp DNA for single-molecule investigations

To experimentally examine the origin localization and dynamics of ORC and MCM on a chromatinized origin of replication, we designed an *in vitro* single-molecule force-fluorescence assay that employed purified yeast proteins (**Supplementary Figure 1.1**). We wished to visualize the chromatinized origin using yeast histone octamers marked with

fluorescent labels. This we achieved by introducing a single cysteine per H2A histone by replacing residue lysine 120 (K120), which avoids disruption of the overall nucleosome structure (**Figure 1a**; Methods). Purified yeast histone octamers containing two H2A (K120C) histones were covalently bound with one single AF488 dye per cysteine (degree of labeling p_{label} = 0.81, as determined from bulk experiments; Methods). We then engineered an ARS1 origin of replication flanked by two nucleosome positioning sequences (NPSs) spaced by 150 bp (50 nm) (Ref. 16 and Methods), and reconstituted fluorescently labeled nucleosomes onto the NPSs using salt gradient dialysis. The resulting chromatinized origin tested positively for *Pst*I restriction digestion between the nucleosomes (**Supplementary Figure 1.2b**), which indicated that it should remain accessible to ORC and MCM. Next, we ligated this chromatinized origin to two biotinylated DNA fragments of distinct sizes. This resulted in a 10.4 kbp chromatinized DNA molecule (**Figure 1b**) in which the origin was localized approximately at one third of the total length of the DNA molecule (**Supplementary Figure 1.2c**). In addition to the ARS1 origin, the 10.4 kbp DNA molecule contained a number of endogenous potential binding sites for ORC[17] and regions of high AT content (**Supplementary Figure 1.2d**).

Following preparation, the 10.4 kbp DNA molecules including a chromatinized origin were introduced into the microfluidic flow cell of our single-molecule instrument. Here, the DNA molecules were tethered to streptavidin-coated beads in a dual-beam optical trap, after which they were visualized in a protein-free channel of the flow cell (buffer channel) while under a tension of 2 pN. Nucleosome-bound AF488-H2A was detected as a bright fluorescent spot (or focus) whose spatial position was determined (**Figure 1b**). By repeating this measurement on multiple DNA molecules, we could build up the spatial distribution of H2A

foci as a function of genomic coordinate. As each individual DNA molecule was tethered in one of two possible orientations in the dual-beam optical trap, we report spatial distributions from the midpoint of the DNA. Each histogram bin (width 0.670 kbp; Methods) thus contains the average of the occupancies of two segments of DNA located symmetrically about the midpoint of the DNA: for example, the origin bin contains the mean of the occupancies of the actual origin- and NPS-containing segment and the DNA segment located oppositely from the midpoint of the DNA by 1.7 kbp. The spatial distribution of H2A fluorescent foci (filtered to remove foci containing more than 4 H2A, which could represent aggregates; Methods) showed a clear peak in the bin containing the NPSs (left panel in **Figure 1c**), suggesting preferential nucleosome assembly at the NPSs. This spatial distribution of H2A was built up from distinct DNA samples chromatinized on different days, which exhibited only minimal differences from one another (**Supplementary Figure 1.4**), highlighting the reproducibility of our sample preparation.

Ideally, our chromatinized origin should contain two fluorescently labeled nucleosomes within a single diffraction-limited spot. Assuming that the identification of a single fluorescently labeled H2A reflects the presence of a single H2A-H2B dimer bound to a H3-H4 tetramer, we should then measure 4 fluorescently labeled H2A per focus. However, the experimental counts of fluorescently labeled H2A may be reduced by non-unity values for the probability of occupancy of the two NPSs ($p_{occupancy}$), the probability of H2A-H2B dimer association to the H3-H4 tetramer (p_{h2a}), and p_{label} **(Supplementary Figure 1.3a**). To count the number of labeled H2A, we identified step-wise photobleaching events using Change-Point Analysis (CPA; Methods), whereby the methodology is assessed and validated using dCas9 tagged and labeled identically to H2A (**Supplementary Figure 1.1**). The lifetime prior to

photobleaching of AF488 when linked to H2A was similar to when it was linked to dCas9, indicating that labeled H2A are stable on the DNA during the experiment (**Supplementary Figure 1.3c**). Using this photobleaching approach, we found that the H2A foci primarily contained two to three AF488-labeled H2A histones, as shown in the stoichiometry distribution (right panel in **Figure 1c**) built up from a total of N_{DNA} = 247 derived from the four different chromatinized DNA samples mentioned above (again exhibiting only minimal differences from one another, **Supplementary Figure 1.4**). With the independently measured p_{label} = 0.81 as fixed parameter, the best fit to the experimentally determined stoichiometry distribution (**Figure 1c**, fitted values described by white numbers inside the bar plot; **Supplementary Figure 1.3b**) yielded $p_{occupancy}$ = 1.00 (corresponding to full occupancy of the NPSs) and p_{h2a} = 0.77.

To confirm that the detected fluorescent H2A foci reflected embedding of H2A into nucleosomes – as opposed to unspecific electrostatic interactions of H2A-H2B dimers with the DNA[18] – we separately probed for nucleosome presence on our 10.4 kbp DNA using force spectroscopy. Previous experiments have shown that under force, DNA can be unwrapped from the histone octamer. Irreversible jumps in the force-extension curve, in which 27 nm (80 bp) of DNA is unwrapped from either a hexasome or a full nucleosome, have been reported to occur over a broad range of forces (8-40 pN) [19-22]. Indeed, when we pulled on one extremity of a tethered chromatinized DNA molecule with labeled H2A histones at a constant speed (100 nm/s) (**Supplementary Figure 1.5a**), we could identify such jumps (**Supplementary Figure 1.5b**). These occurred at a force of 17.6 pN ± 5.8 pN (mean ± standard deviation) and yielded contour length increments of 24.8 nm ± 5.9 nm (mean ± standard deviation), the latter corresponding to the contour length of the unwrapped DNA. At least two such jumps were

revealed in 88.5% of the DNA molecules (**Supplementary Figure 1.5c**), implying that our chromatinized DNA typically contains two nucleosomes (or hexasomes).

Together, these single-molecule fluorescence and force spectroscopy results support our establishment of a 10.4 kbp DNA containing a single origin of replication flanked by two nucleosomes. As the force spectroscopy does not report on nucleosome location, however, to investigate the influence of a chromatinized origin of replication on ORC and MCM, we focused on fluorescence readouts alone.

Nucleosomes enhance intrinsic ORC preference for the origin of replication

To study the effect of chromatinized origins on ORC binding and dynamics, we labeled the N-terminus of the Orc3 subunit with a JF646 fluorophore via a HaloTag (Methods). We confirmed that the labeled ORC could load MCM in bulk assays (**Supplementary Figure 1b**). We then prepared four different 10.4 kbp DNA molecules that either contained ARS1 or a mutated origin without specific affinity for ORC[15, 23], and that were chromatinized or not.

We first performed experiments that report on the rapid binding of ORC to a chromatinized origin. To do so, we incubated the optically trapped DNA molecule held at near-zero force in a reservoir of the microfluidic flowcell that contained 5 nM JF646-ORC for 5 s. Subsequently, we shifted the DNA to a separate, protein-free channel and imaged it under a stretching force of 2 pN (**Figure 2a**). DNA-bound JF646-ORC was observed as a bright fluorescent spot (focus); foci containing more than 5 ORCs, which could represent aggregates (Methods), were not analyzed further. Stoichiometric analysis of the foci via step-wise photobleaching indicated that they predominantly contained individual ORC molecules (**Supplementary Figure 2**).

Fluorescent foci were observed throughout the DNA molecule, but the overall spatial distribution exhibited clear overrepresentation of ORC in the bin containing the ARS1 origin (30% of the total, **Figure 2b-i**). This preference for ORC binding in the bin containing the origin[15] increased to 39% when the origin was chromatinized (**Figure 2b-ii**). Mutation of the origin reduced preferential binding by ORC in the bin containing the origin[15]; instead, ORC was observed to peak in an adjacent bin (**Figure 2b-iii**) that included a potential ORC binding site (located at 2.4 kbp from the start of the construct, **Supplementary Figure 1.2d**). Chromatinization of this mutated origin nonetheless increased ORC presence in the origin bin from 14% to 26% (**Figure 2b-iii, 2b-iv**). For the four conditions probed, ORC binding in the bin containing the origin (chromatinized or not) was subjected to tests of statistical significance (**Figure 2c**). These results indicate statistically significant enhancement of ORC binding given either the presence of ARS1 or the presence of nucleosomes, with the effect of the former being more pronounced.

Nucleosomes flanking the origin reduce ORC mobility and increase ORC lifetime

We have previously shown that ORC is a mobile protein that slides on bare DNA[15]. Here we sought to investigate ORC dynamics on DNA containing a chromatinized origin following rapid binding under the incubation conditions described above (**Figure 2a**). When we tracked the position of ORC molecules initially located in the bin containing the chromatinized origin over time (**Figure 3a-i**, showing 30% of all traces, selected at random), it appeared that within experimental error many of these ORC molecules hardly changed their position over time. Conversely, ORC molecules initially located outside the origin (**Figure 3a-ii**, showing 30% of all traces, selected at random) were observed to explore their local DNA environment in

seemingly random fashion, which in some cases allowed them to approach, and then move away from, the nucleosomes.

To quantify this dynamic behavior of ORC, we calculated the mean squared displacement for each ORC molecule on the four types of DNA molecules described above versus time interval and extracted a diffusion constant from a linear fit. Distributions (in log scale) of the fitted diffusion constants are shown in **Figure 3b**. We observed a wide spread of diffusion constants, ranging from 10^{-6} to 10^{0} kbp^2 s^{-1}. Using the Bayesian Information Criterion, we identified kinetically distinct population states for ORC on non-chromatinized DNA containing ARS1 (**Figure 3b-i**). These describe either a population with low mean diffusion constant (hereafter 'slow ORC population') (D_{slow} = 0.0049 ± 0.0028 kbp^2 s^{-1} (mean ± SEM)) and a population with a higher mean diffusion constant (hereafter 'fast ORC population') (D_{fast} = 0.152 ± 0.023 kbp^2 s^{-1}), consistent with our earlier findings for ORC on longer DNA molecules that contained a synthetic origin of replication[15]. We used these means as imposed values in fitting the distribution of ORC diffusion constants obtained on the other three types of DNA molecules (**Figure 3b-ii, 3b-iii, and 3b-iv**). As one can observe both by eye and from the fits, chromatinization of the ARS1 origin resulted in an increase in the slow ORC population (Figure 3b-ii). On DNA molecules with the mutated origin, the fast ORC population predominated **(Figure 3b-iii**), again consistent with our previous findings[15], but chromatinization of this mutated origin also resulted in an increase in the slow ORC population (**Figure 3b-iv**). We summarize these results more quantitatively by computing the fraction of the slow ORC population in the total, whereby we used the geometric mean D^* (= 10 ^ ([μ_{slow} + μ_{fast}]/2) = 0.0065 kbp^2 s^{-1}, with μ_i the lognormal population means) as a cutoff (**Figure 3c-i**). This fraction was always observed to be higher upon chromatinization of the origin.

To assess how chromatinization of the origin resulted in an increase of the slow ORC population, we repeated this analysis separately for ORC molecules initially localized in the origin bin (**Figure 3c-ii**) and for ORC molecules initially localized elsewhere (**Figure 3c-iii**). For ORC molecules initially localized in the origin bin, chromatinization of the origin led to an increase in the slow ORC population, irrespective of whether the origin contained ARS1 or was mutated (**Figure 3c-ii**). This reduction in ORC mobility could have resulted solely from the spatial confinement imposed on ORC by the nucleosomes, or additionally through ORC interactions with the nucleosomes. Interestingly, for ORC molecules initially localized elsewhere, chromatinization of the origin also led to an increase in the slow population of ORC molecules, again irrespective of the origin contained ARS1 or was mutated (**Figure 3c-iii**). This reduction in ORC mobility suggested ORC interactions with the nucleosomes.

To address whether chromatinization of the origin influenced the stability of ORC binding, we examined the lifetimes of individual JF646 dyes on DNA-bound ORC molecules by tracking foci containing 1 or 2 ORC molecules at 0.6 s/frame until the fluorescence signal disappeared. Apart from on the DNA molecule with the chromatinized mutated origin, the mean lifetime of ORC was shorter than 30 s, making it substantially shorter than the bleaching-limited mean lifetime of JF646 measured under identical imaging conditions (71.0 s, **Supplementary Figure 1.1c**) by attaching it to DNA-bound dCas9. This indicated that ORC molecules typically dissociated from DNA during the measurement, in accord with our previous observations[15]. Nonetheless, the mean lifetime of the slow ORC population typically exceeded that of the fast ORC population (**Supplementary Figure 3b**). Of the ORC molecules initially located at or close to the ARS1 origin on bare DNA, 61% were associated with the slow ORC population (red bin,

Figure 3c-ii); this fraction is increased to 84% upon chromatinization of the ARS1 origin ('bordeaux' bin, **Figure 3c-ii**). While not all of these ORC molecules may be specifically bound to DNA (as also suggested by a corresponding increase in the slow ORC population observed upon chromatinization of the mutated origin, compare grey and pink bins in **Figure 3c-ii**), nonetheless the increase in the slow ORC population with its higher mean lifetime on a chromatinized ARS1 suggests that flanking nucleosomes can contribute to the temporal retention of ORC near an origin of replication. This could in turn contribute to preferential recruitment of MCM there.

Stable ORC binding to DNA requires the origin of replication

We also performed experiments with more extended incubation conditions compatible with the timescale required for full maturation of MCM[5, 15]. When performed with ORC and Cdc6 only (next section for experiments involving MCM), these experiments provided a read-out of long-lived, stable ORC binding. Concretely, we incubated ORC and Cdc6 in bulk, for 30 min with the four types of DNA molecules (untethered to beads, hence with free ends), prior to imaging in single-molecule conditions. We separately verified that an extended incubation period alone did not affect the distributions of H2A position or stoichiometry on chromatinized DNA (**Supplementary Figure 4.1**). We then introduced these pre-incubated DNA molecules into the flowcell, trapped them, and imaged stable ORC molecules that remained bound to the DNA (**Figure 4a**).

Following this experimental approach, on bare DNA molecules containing the ARS1 origin we observed either DNA molecules devoid of ORC ($N_{DNA\text{-}no\ ORC}$ = 10, 21% of total), or DNA molecules ($N_{DNA\text{-}ORC}$ = 38, 79% of total) with ORC. Using the latter, we plotted the spatial

distribution of ORC (**Figure 4b-i**). We found that 61% of the ORC foci were localized in the origin bin (N_{foci} = 38, $N_{foci\ in\ origin}$ = 23), which emphasizes the stability of ORC binding to the origin compared to the other DNA sequences in the 10.4 kbp DNA[15]. Stoichiometric analysis showed no difference with the experiments reporting on rapid ORC binding (compare **Supplementary Figure 2b-i** and **Supplementary Figure 4.2b-i**). On DNA molecules with a chromatinized ARS1 origin, the overall fraction of DNA molecules containing ORC foci was reduced by a factor of two, to 41% ($N_{DNA\text{-}no\ ORC}$ = 74, $N_{DNA\text{-}ORC}$ = 52). However, we observed a similar fraction (51%) of ORC foci localized in the origin bin (N_{foci} = 43, $N_{foci\ in\ origin}$ = 22, **Figure 4b-ii**), indicating that chromatinization of ARS1 did not enhance the likelihood of finding ORC stably bound in the origin bin relative to elsewhere on the DNA. Interestingly, stoichiometric analysis showed an increase in the number of ORC molecules per focus (**Supplementary Figure 4.2b-ii**). When these experiments were repeated on DNA molecules with the mutated origin, we predominantly found DNA molecules devoid of ORC, irrespective of whether nucleosomes were present ($N_{DNA\text{-}no\ ORC}$ = 45, $N_{DNA\text{-}ORC}$ = 2, **Figure 4b-iv**) or not ($N_{DNA\text{-}no\ ORC}$ = 32, $N_{DNA\text{-}ORC}$ = 10, **Figure 4b-iii**). This suggested that stable ORC binding probed under these experimental conditions is predominantly associated with DNA sequence. For the four conditions probed, ORC binding in the bin containing the origin (chromatinized or not) was subjected to tests of statistical significance (**Figure 4c**). These results indicate statistically significant enhancement of stable ORC binding that depends on the presence of ARS1, but not on the presence of chromatin.

Previous studies have shown direct interactions between ORC and nucleosomes, suggesting a potential for nucleosome remodeling by ORC[26, 29]. Thus, we assessed whether in our experiments the presence of ORC and Cdc6 impacted the spatial distribution and

stoichiometry of H2A. For reference, following a 30 min buffer-only bulk incubation of the DNA with a chromatinized ARS1 origin (N_{DNA} = 51), 80% of H2A foci were found in the origin bin (N_{foci} = 45, $N_{foci\ in\ origin\ bin}$ = 36), and the best fit of the H2A stoichiometry distribution yielded p_{h2a} = 0.73 and $p_{occupancy}$ = 0.98 (**Supplementary Figure 4.1**), similar to the lack of incubation (**Figure 1c)**. When the bulk incubation was performed in the presence of ORC and Cdc6 (N_{DNA} = 126), however, the fraction of H2A foci in the origin bin was reduced to 49% (N_{foci} = 134, $N_{foci\ in\ origin\ bin}$ = 66) (**Supplementary Figure 4.3b**), and the best fit of the H2A stoichiometry distribution yielded p_{h2a} = 0.81 and $p_{occupancy}$ =0.52. The latter parameters suggested a maintenance of H2A-H2B dimer stability but a less complete NPS occupancy. When the bulk incubation in the presence of ORC and Cdc6 was performed on DNA molecules with a chromatinized mutated origin (N_{DNA} = 47), an intermediate value of 64% of H2A foci were found in the origin bin (N_{foci} = 56, $N_{foci\ in\ origin\ bin}$ = 36) (**Supplementary Figure 4.3c**), and the best fit of the H2A stoichiometry distributions of H2A yielded p_{h2a} = 0.60 and $p_{occupancy}$ = 1.00. The latter parameters indicated a reduction in H2A-H2B dimer stability without a change in NPS occupancy. In summary, these results show that under these more extended incubation conditions, the presence of ORC and Cdc6 can influence nucleosome positioning and stability.

Nucleosomes flanking the origin permit MCM recruitment but restrict subsequent motion

Having probed both rapid and stable ORC binding and established that the presence of ARS1 was beneficial to both but the presence of nucleosomes only to the former, we wanted to test how the presence of nucleosomes impacted the loading of MCM. We therefore set out to probe the spatial positioning, stoichiometry, and dynamics of MCM on a chromatinized origin. To visualize MCM, we used JF646-labeled MCM in loading reactions. MCM was labeled by introducing a HaloTag on the N-terminus of its Mcm3 subunit, and JF646-MCM performed

normally in a bulk loading assay (**Supplementary Figure 1.1**). We then incubated ORC, Cdc6 and MCM/Cdt1 with DNA in bulk, without tethering to beads, for 30 min[5, 15] as described above for the experiments that probed for stable ORC binding. We next introduced these pre-incubated DNA molecules into the flow cell, and imaged JF646-MCM as described above (**Figure 5a**).

In the absence of nucleosomes, MCM foci were broadly distributed about the ARS1 origin (**Figure 5b-i**), as previously described[15]. Chromatinization of ARS1 origin, however, resulted in a strikingly different situation: MCM foci were now mainly localized in the origin bin (**Figure 5b-ii**). Repeating this experiment on bare DNA containing the mutated origin again resulted in a broad distribution of MCM (**Figure 5b-iii**), this time with a slight peak in the same bin as was observed in the experiments that probed rapid ORC binding (**Figure 2b-iii**). Chromatinization of this mutated origin did not significantly increase the presence of MCM in the origin bin (**Figure 5b-iv**). For the four types of DNA molecules probed, MCM binding in the bin containing the origin (chromatinized or not) was subjected to tests of statistical significance (**Figure 5c**). These results indicate that chromatinization of the ARS1 origin, but not of a DNA segment without ARS1, statistically significantly increases the population of MCM bound there.

We also examined the stoichiometry of MCM foci bound to four different types of DNA molecules tested under these four conditions. Stoichiometric analysis showed that the MCM foci predominantly contained 1 or 2 molecules for all cases (**Supplementary Figure. 5.1**). However, foci found on DNA molecules that contained the chromatinized ARS1 origin exhibited the highest fraction of foci in the origin bin that contained 2 MCM molecules (53%,

right plot in **Supplementary Figure 5.1-ii**). We discuss this further below, together with the overall observation that the spatial distributions of MCM resembled those obtained for rapid ORC binding more closely than those obtained for stable ORC binding.

As our experiments showed that the presence of ORC and Cdc6 during 30 min incubations in bulk impacted nucleosome positioning and stability (**Supplementary Figure 4.3**), we also monitored nucleosome positioning and stability upon the inclusion of MCM. On DNA molecules with a chromatinized ARS1 (N_{DNA} = 110), 83% of H2A foci were found in the origin bin (N_{foci} = 81, $N_{foci\ in\ origin\ bin}$ = 67), and the best fit of the H2A stoichiometry distribution yielded p_{h2a} = 0.84 and $p_{occupancy}$ = 0.89 (**Supplementary Figure 5.2b**), which are all values similar to those obtained following incubation with buffer alone. However, on DNA with a chromatinized mutated origin (N_{DNA} = 123), only 50% of H2A foci were located in the origin bin (N_{foci} = 70, $N_{foci\ in\ origin\ bin}$ = 140), and the best fit of the H2A stoichiometry distribution yielded p_{h2a} = 0.91 and $p_{occupancy}$ = 0.40. The latter parameters suggested a maintenance of H2A-H2B dimer stability but a less complete NPS occupancy. We speculate that increased MCM loading on a chromatinized ARS1 origin (**Supplementary Figure 5.2a**) relative to the chromatinized mutated origin (**Supplementary Figure 5.2b**) limits the continued access of ORC and Cdc6 to nucleosomes, and hence their impact (see also Discussion).

Lastly, we tested whether a pair of nucleosomes surrounding ARS1 can prevent MCM, once loaded, from diffusing outwards away from ARS1. To test this directly, we monitored MCM position over an extensive duration of time by repeated the preceding experiments but imaging JF646-MCM at a 100-fold slower rate (one frame per min, **Figure 5d**). This allowed us to probe for MCM motion occurring on timescales up to approximately 15 min. We measured

the relative displacements of JF646-MCM foci every 2 min (or 2 frames) until JF646 was no longer visible due to photobleaching (lifetime of the JF646 dye on DNA-bound dCas9 under identical imaging conditions was 1236.0 s). These data were benchmarked relative to the displacement distribution of dCas9 (Figure 5e-i) obtained under identical experimental conditions, which was centered about 0 and had a width of σ = 0.061 kbp that derived from experimental noise. The distribution of displacements by MCM on DNA molecules with a bare ARS1 had a substantially increased width relative to dCas9 (Figure 5f-ii; σ = 0.398 kbp), indicating one-dimensional diffusion of the MCM foci as previously observed[15]. However, on DNA containing the chromatinized ARS1, the distribution of displacements by MCM had a narrow width (Figure 4f-iii; σ = 0.153 kbp). This indicated that the one-dimensional diffusion of MCM was constrained by the presence of nucleosomes flanking the ARS1 origin of replication.

DISCUSSION

Chromatin replication starts from origins that are flanked by nucleosomes. We have studied the behavior of yeast replication proteins at the single-molecule level to understand how the presence of nucleosomes impacts the binding and mobility of ORC in the vicinity of the origin and subsequently, the recruitment and mobility of MCM.

Nucleosomes facilitate rapid binding of ORC to the origin and decrease its mobility

We probed the level of rapid binding of yeast ORC to DNA following a short incubation period in the single-molecule instrument and observed a mild increase in the region containing the ARS1 origin in the presence of flanking nucleosomes (**Figure 2b, c**). A similar effect was observed in control experiments on DNA molecules containing a mutated origin (**Figure 2d,**

e). The subsequent mobility of these ORC molecules was monitored by following their displacement over time and computing a diffusion constant for each acquired trace. Histograms of such diffusion coefficients showed that the prevalence of a slow population of ORC molecules significantly increased in the presence of nucleosomes flanking ARS1, regardless of whether a given ORC molecule was originally positioned within or outside of the region containing the ARS1 origin (**Figure 3b, c**). Nucleosomes flanking a mutated origin result in a similar reduction on the mobility of ORC (**Figure 3d, e**). Thus, the presence of nucleosomes provides a mild increase in local ORC binding and a reduction in ORC mobility, where the latter can derive from spatial confinement of ORC by nucleosomes and/or direct interactions between ORC and nucleosomes. Direct interactions between ORC and nucleosomes could account for the increase in local ORC binding if nucleosomes similarly affected both the influx and efflux of mobile ORC molecules onto the origin region. How, then, do we view the role of ORC mobility overall? Mobile ORC molecules can contribute to origin recognition by scanning the DNA – given the measured diffusion constant of the fast ORC population, even during a short 5 s incubation period an individual ORC molecule can scan ~1.2 kbp on bare DNA, which contributes to its observed binding at many different sites along the DNA (**Figure 2b**). Our data show that in the yeast system ORC molecules can readily locate a chromatinized origin via binding from solution even if the 1D diffusive pathway is blocked; whether the same holds true for higher eukaryotes that lack origins with clear sequence preference remains to be determined.

Stable binding of ORC is primarily enabled by the origin of replication

We next asked whether nucleosomes affected the stable binding of ORC to DNA following bulk incubation of ORC with DNA molecules over an extended duration. Examination in the

single-molecule instrument revealed that a bare ARS1 origin alone sufficed to retain stably bound ORC molecules to DNA (**Figure 4a**); no further increases in the yield of stable ORC were observed with a chromatinized ARS1 origin (**Figure 4b**). Interestingly, while DNA molecules that contained a mutated origin could recruit rapidly bound ORC (**Figure 2d,e**), they could not stably retain ORC, irrespective of whether nucleosomes surrounded the origin (**Figure 4d,e**). This comparison suggests that ORC molecules that are rapidly but nonspecifically recruited, can exit a segment of DNA flanked by nucleosomes. As our direct tracking of the motion of ORC does not provide experimental evidence that ORC can bypass flanking nucleosomes (**Figure 3**), such ORC molecules must then unbind from the DNA directly into solution[30]. Our finding that stable ORC binding depends on the presence of ARS1 contrasts with a published report based on a different *in vitro* approach for loading nucleosomes onto single molecules of DNA that suggested that nucleosomes facilitated ORC binding independently of DNA sequence[26]. It is, however, in line with studies of yeast replication *in vitro* on chromatinized DNA and *in vivo* in budding yeast that indicate a requirement for the presence of origin sequences[27, 28].

Stoichiometric analysis of either rapidly or stably bound ORC molecules in the region containing the ARS1 origin indicated an increase in ORC stoichiometry upon chromatinization (**Supplementary Figure 2**). We computed the resulting ratio of 1 ORC molecule:2 ORC molecules to be ~1:3, very similar to the ratio previously determined using cryo-EM[16]. An increase in ORC stoichiometry upon chromatinization of ARS1 could result from a similar influx of ORC to the origin but a reduced efflux as the diffusion of ORC molecules away from the origin[15] is reduced by the presence of nucleosomes, or an increased influx of ORC to the

origin due to direct interactions between ORC and nucleosomes[26, 29], or a combination of these effects.

Influence of ORC and MCM on nucleosome remodeling at the origin of replication

Previous studies have indicated that ORC has properties of a chromatin remodeler[12-14, 24], either due to direct interaction of ORC with the nucleosomes or due to DNA bending at the origin[31]. Indeed, we confirmed that extended incubation of chromatinized substrates with ORC and Cdc6 could broaden the spatial distribution and/or reduce the stoichiometry of the H2A histones embedded within our nucleosomes (**Supplementary Figure 4.3**), in agreement with published work reporting in vitro remodeling of H2A-H2B dimers by ORC[24]. However, our position and stoichiometry distributions of H2A indicated that its remodeling is reduced when loading of MCM is enabled. This suggests a protective role for MCM in the maintenance of epigenetic chromatin states prior to the firing of DNA replication[32].

Loading of MCM onto a chromatinized origin

Our results showed that the lack of a replication origin inhibits the stable binding of ORC to DNA (**Figure 4**), but not the rapid binding of ORC (**Figure 2**) or the loading of MCM (**Figure 5**). This implies that stable binding of ORC at ARS1 is not a prerequisite to MCM loading, which is consistent with biochemical experiments showing that MCM loading can occur independently of specific origins[5]. Furthermore, our measurements of the spatial distributions of MCM indicate that for the four types of DNA molecules tested, there is a probability of finding MCM molecules all along the DNA molecule. Several factors are underlying this behavior. First, it is the one just mentioned: ORC binding is not strictly sequence-specific even in yeast, and thus MCM loading can occur at different DNA sequences. Indeed, the spatial distribution of MCM

molecules (**Figure 5**) showed similar features to the spatial distributions of rapid ORC binding (**Figure 2).** Second, both bulk biochemical assays[4, 5] and our previous single-molecule studies[15] have shown that loaded MCM can undergo linear diffusion on DNA. In the buffer conditions employed, the diffusion constant of MCM equals 0.0008 ± 0.0002 $kbp^2\ s^{-1}$ (**Figure 5e-ii**), from which we estimate that diffusion of MCM during the extended incubation period contributed ~1.4 kbp to the broadening of its spatial distribution.

On DNA molecules containing a chromatinized ARS1, we found that the probability of finding MCM proteins in the vicinity of the origin was increased by more than two-fold compared to that on DNA molecules containing bare ARS1. Given that chromatinizing ARS1 increases the probability of MCM foci close to the origin (**Figure 5c**) more than the probability of finding rapidly bound ORC foci close to the origin (**Figure 2c**), this suggests that the presence of nucleosomes prevents the diffusion of MCM molecules away from the origin. The lack of a similar increase in the probability of MCM foci close to the origin due to the chromatinization of a mutated origin, compare **Figure 4e** to **Figure 4d** (despite a corresponding mild increase in rapid ORC binding, compare **Figure 2e** to **Figure 2d**) is consistent with previous work showing that nucleosomes reduced the non-specific loading of MCM on a mutated origin[13,33].

Stoichiometric analysis reveals that the detected MCM foci in region of the ARS1 origin predominantly have a stoichiometry of 1 or 2. In the presence of the nucleosomes, however, we clearly observed more foci with a stoichiometry of 2 (**Supplementary Figure 5.1b**). While in our experimental configuration a measured MCM stoichiometry of 2 within a diffraction-limited focus does not distinguish between an MCM double hexamer and two single MCM hexamers, our results are consistent with previous work showing that a chromatinized ARS1

origin favors the formation of the MCM/ORC (MO) intermediate complex and, consequently, the loading of MCM double hexamers[16].

MCM is spatially constrained to a chromatinized origin on long timescales

It has been speculated that MCM could potentially displace or remodel nucleosomes. Our data monitoring the position and stoichiometry distributions of H2A following an extended incubation with all loading factors, however, show no changes therein on DNA containing a chromatinized ARS1 origin (**Supplementary Figure 5.2**). Our experimental tracking of MCM position over long incubation times confirms this directly by establishing that the presence of nucleosomes spatially constrains MCM (**Figure 5e**). Potentially, the presence of MCM spatially constrained between nucleosomes could facilitate replisome assembly on the origin of replication. However, if nucleosomes can function as roadblocks for MCM diffusion as we have shown, then they could also function as roadblocks to single MCM hexamers and thereby reduce the likelihood of double MCM double hexamer formation through this pathway[23]. However, the presence of origin-flanking nucleosomes has been shown to favor pre-RC formation[11, 12]. Therefore, it appears that in yeast the presence of origin-flanking nucleosomes is key. This would predict a reduced initiation of DNA replication at nonspecific locations under regular chromatin packaging conditions[34], which could potentially be relaxed at transcription-replication conflicts or under conditions of DNA replication stress[35, 36].

Conclusions

Our findings provide new insights into the role of chromatin in DNA replication initiation. We demonstrate that the presence of nucleosomes surrounding origins contributes to the loading and subsequent spatial constraint of MCM hexamers there, thereby presumably favoring

CMG formation and the initiation of DNA replication at replication origins. The implications that nucleosomes act as barriers to MCM diffusion will be further investigated, as we anticipate that they could play a relevant role in the recycling of licensing factors in cases of DNA replication stress, where reloading of factors is not possible. This research will open up new avenues to further explore the role of chromatin in origin firing and the mechanisms of chromatin replication.

REFERENCES

1. Bellush JM, Whitehouse I. DNA replication through a chromatin environment. *Philos Trans R Soc Lond B Biol Sci* **372**, (2017).
2. Bell SP, Labib K. Chromosome Duplication in Saccharomyces cerevisiae. *Genetics* **203**, 1027-1067 (2016).
3. Bell SP, Stillman B. ATP-dependent recognition of eukaryotic origins of DNA replication by a multiprotein complex. *Nature* **357**, 128-134 (1992).
4. Evrin C*, et al.* A double-hexameric MCM2-7 complex is loaded onto origin DNA during licensing of eukaryotic DNA replication. *Proc Natl Acad Sci U S A* **106**, 20240-20245 (2009).
5. Remus D, Beuron F, Tolun G, Griffith JD, Morris EP, Diffley JF. Concerted loading of Mcm2-7 double hexamers around DNA during DNA replication origin licensing. *Cell* **139**, 719-730 (2009).
6. Douglas ME, Ali FA, Costa A, Diffley JFX. The mechanism of eukaryotic CMG helicase activation. *Nature* **555**, 265-268 (2018).
7. Ramirez Montero D*, et al.* Nucleotide binding halts diffusion of the eukaryotic replicative helicase during activation. *Nat Commun* **14**, 2082 (2023).
8. Yeeles JT, Deegan TD, Janska A, Early A, Diffley JF. Regulated eukaryotic DNA replication origin firing with purified proteins. *Nature* **519**, 431-435 (2015).
9. Yeeles JTP, Janska A, Early A, Diffley JFX. How the Eukaryotic Replisome Achieves Rapid and Efficient DNA Replication. *Mol Cell* **65**, 105-116 (2017).
10. Venditti P, Costanzo G, Negri R, Camilloni G. ABFI contributes to the chromatin organization of Saccharomyces cerevisiae ARS1 B-domain. *Biochim Biophys Acta* **1219**, 677-689 (1994).
11. Eaton ML, Galani K, Kang S, Bell SP, MacAlpine DM. Conserved nucleosome positioning defines replication origins. *Genes Dev* **24**, 748-753 (2010).
12. Lipford JR, Bell SP. Nucleosomes positioned by ORC facilitate the initiation of DNA replication. *Mol Cell* **7**, 21-30 (2001).
13. Azmi IF*, et al.* Nucleosomes influence multiple steps during replication initiation. *Elife* **6**, (2017).
14. Chacin E*, et al.* Establishment and function of chromatin organization at replication origins. *Nature*, (2023).

15. Sanchez H*, et al.* DNA replication origins retain mobile licensing proteins. *Nat Commun* **12**, 1908 (2021).
16. Miller TCR, Locke J, Greiwe JF, Diffley JFX, Costa A. Mechanism of head-to-head MCM double-hexamer formation revealed by cryo-EM. *Nature* **575**, 704-710 (2019).
17. Liachko I, Youngblood RA, Keich U, Dunham MJ. High-resolution mapping, characterization, and optimization of autonomously replicating sequences in yeast. *Genome Res* **23**, 698-704 (2013).
18. Andrews AJ, Chen X, Zevin A, Stargell LA, Luger K. The histone chaperone Nap1 promotes nucleosome assembly by eliminating nonnucleosomal histone DNA interactions. *Mol Cell* **37**, 834-842 (2010).
19. Brower-Toland BD, Smith CL, Yeh RC, Lis JT, Peterson CL, Wang MD. Mechanical disruption of individual nucleosomes reveals a reversible multistage release of DNA. *Proc Natl Acad Sci U S A* **99**, 1960-1965 (2002).
20. Diaz-Celis C*, et al.* Assignment of structural transitions during mechanical unwrapping of nucleosomes and their disassembly products. *Proc Natl Acad Sci U S A* **119**, e2206513119 (2022).
21. Mihardja S, Spakowitz AJ, Zhang Y, Bustamante C. Effect of force on mononucleosomal dynamics. *Proc Natl Acad Sci U S A* **103**, 15871-15876 (2006).
22. Sheinin MY, Li M, Soltani M, Luger K, Wang MD. Torque modulates nucleosome stability and facilitates H2A/H2B dimer loss. *Nat Commun* **4**, 2579 (2013).
23. Coster G, Diffley JFX. Bidirectional eukaryotic DNA replication is established by quasi-symmetrical helicase loading. *Science* **357**, 314-318 (2017).
24. Li S, Wasserman MR, Yurieva O, Bai L, O'Donnell ME, Liu S. Origin recognition complex harbors an intrinsic nucleosome remodeling activity. *Proc Natl Acad Sci U S A* **119**, e2211568119 (2022).
25. Berbenetz NM, Nislow C, Brown GW. Diversity of eukaryotic DNA replication origins revealed by genome-wide analysis of chromatin structure. *PLoS Genet* **6**, e1001092 (2010).
26. Li S, Wasserman MR, Yurieva O, Bai L, O'Donnell ME, Liu S. Nucleosome-directed replication origin licensing independent of a consensus DNA sequence. *Nat Commun* **13**, 4947 (2022).
27. Devbhandari S, Jiang J, Kumar C, Whitehouse I, Remus D. Chromatin Constrains the Initiation and Elongation of DNA Replication. *Mol Cell* **65**, 131-141 (2017).
28. Marahrens Y, Stillman B. A yeast chromosomal origin of DNA replication defined by multiple functional elements. *Science* **255**, 817-823 (1992).
29. De Ioannes P*, et al.* Structure and function of the Orc1 BAH-nucleosome complex. *Nat Commun* **10**, 2894 (2019).
30. Speck C, Stillman B. Cdc6 ATPase activity regulates ORC x Cdc6 stability and the selection of specific DNA sequences as origins of DNA replication. *J Biol Chem* **282**, 11705-11714 (2007).
31. Li N*, et al.* Structure of the origin recognition complex bound to DNA replication origin. *Nature* **559**, 217-222 (2018).
32. Petryk N*, et al.* MCM2 promotes symmetric inheritance of modified histones during DNA replication. *Science* **361**, 1389-1392 (2018).
33. Kurat CF, Yeeles JTP, Patel H, Early A, Diffley JFX. Chromatin Controls DNA Replication Origin Selection, Lagging-Strand Synthesis, and Replication Fork Rates. *Mol Cell* **65**, 117-130 (2017).

34. Lee W*, et al.* A high-resolution atlas of nucleosome occupancy in yeast. *Nat Genet* **39**, 1235-1244 (2007).
35. Gros J, Kumar C, Lynch G, Yadav T, Whitehouse I, Remus D. Post-licensing Specification of Eukaryotic Replication Origins by Facilitated Mcm2-7 Sliding along DNA. *Mol Cell* **60**, 797-807 (2015).
36. Scherr MJ, Wahab SA, Remus D, Duderstadt KE. Mobile origin-licensing factors confer resistance to conflicts with RNA polymerase. *Cell Rep* **38**, 110531 (2022).

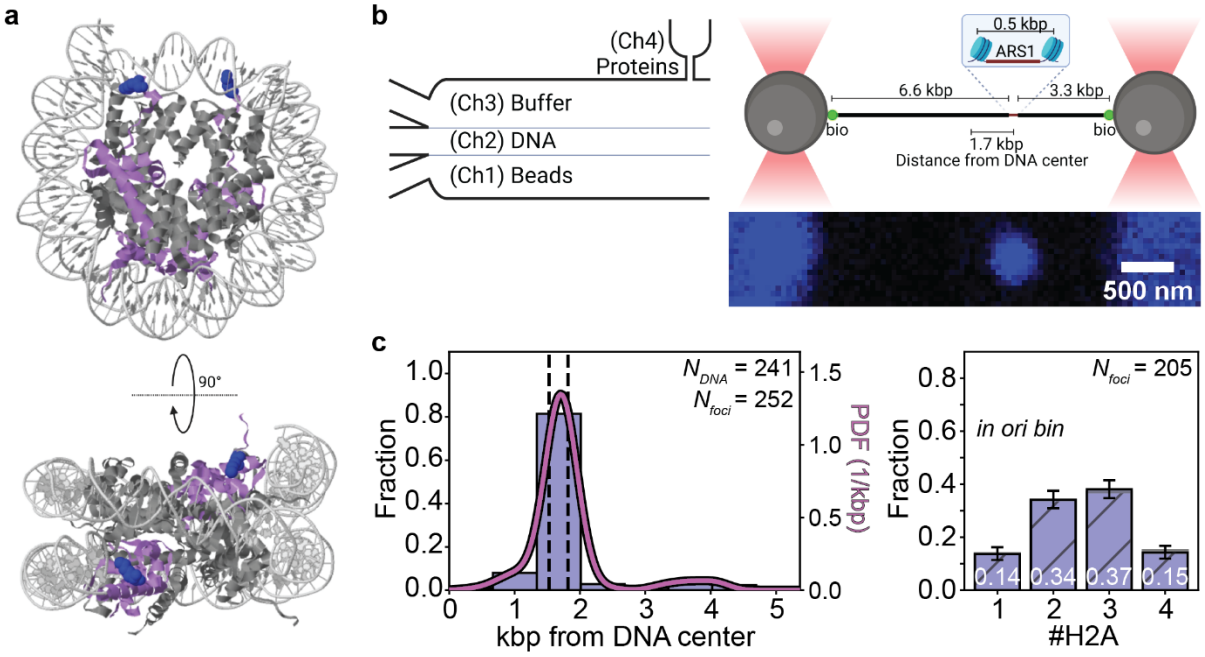

Figure 1. Design and characterization of a labeled chromatinized origin within 10.4 kbp DNA. **(a)** Structural depictions of the yeast nucleosome (PDB: 1ID3), including in blue the mutated residues on the H2A histones for adding fluorescent labels. **(b)** (left panel) Schematic of the flow cell used in the single-molecule experiments. (right upper panel) Schematic of the 10.4 kb DNA held in an optical trap that contains the ARS1 origin of replication flanked by two nucleosome positioning sites (NPSs). The DNA is chromatinized via salt gradient dialysis prior to its introduction into the single-molecule flow cell (**Supplementary Figure 1.2**). (right lower panel) Confocal scan showing that signal from fluorescently labeled H2A histones is detected as a single diffraction-limited spot localized at the NPSs. **(c)** (left panel) Spatial distribution of fluorescently labeled H2A on DNA described in panel (b), as deduced from the blue diffraction-limited spots (N_{foci}) collected from 248 distinct DNA molecules (N_{DNA}). Dashed lines indicate the location of the NPSs, and the solid curve indicates the kernel density estimation of the data. (right panel) Stoichiometry distribution of fluorescently labeled H2A histones in the bin containing the chromatinized origin. Error bars are one-sigma Wilson confidence

intervals. White numbers inside the bars designate the fitted values based on the model described in the Methods and in **Supplementary Figure 1.3**. Data in both panels derives from four chromatinized samples (**Supplementary Figure 1.4**).

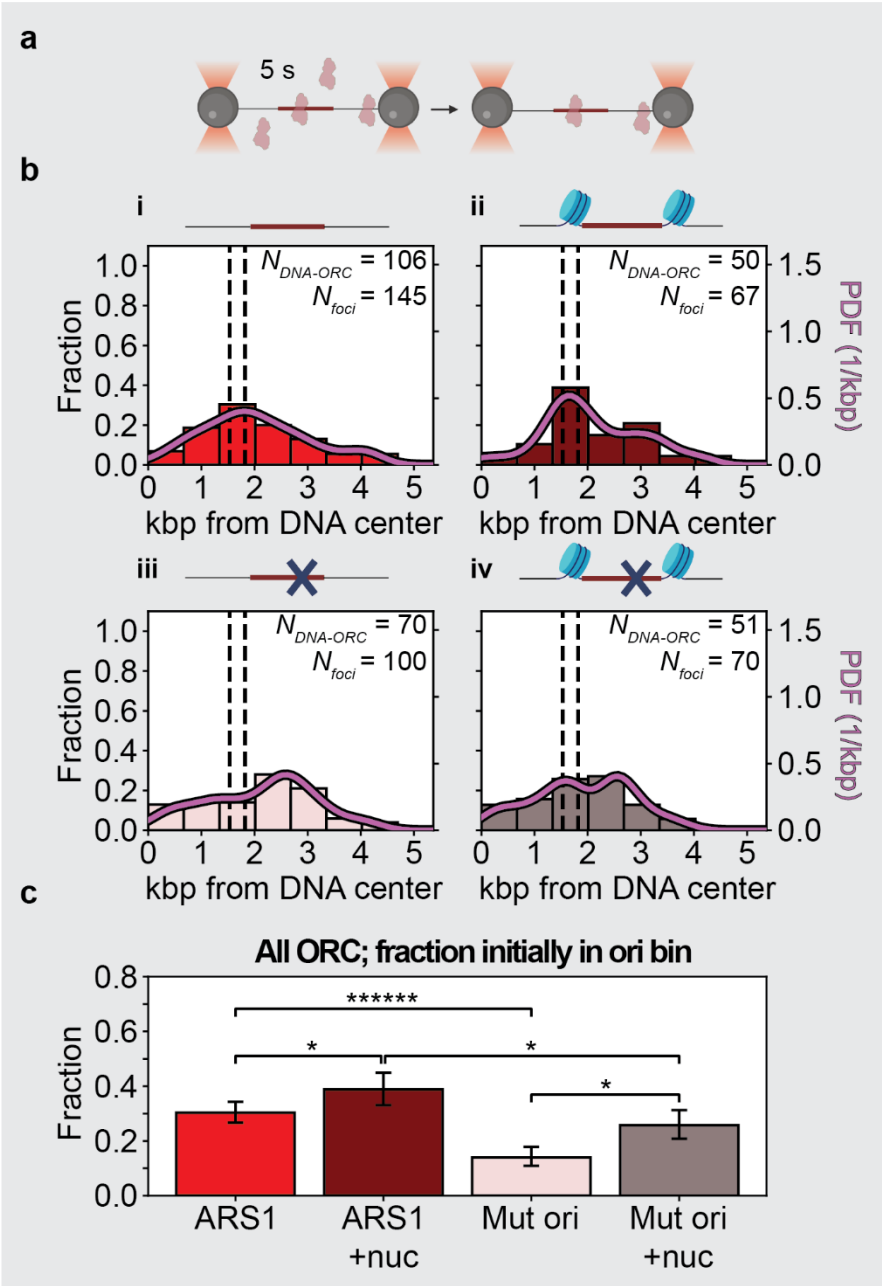

Figure 2. Spatial distribution of rapidly bound ORC on 10.4 kbp DNA containing a chromatinized origin. (a) Incubation method pertaining to data in panels (b-c). Tethered DNA molecules (chromatinized or not, as indicated) are introduced into protein channel (Ch4) for incubation with ORC and Cdc6 for 5 s in the presence of ATP, and then moved into the buffer channel (Ch3) for confocal scanning (see **Figure 1b** for schematic of the flow cell). **(b)** (i) Spatial distribution of ORC on DNA containing a non-chromatinized origin as deduced from the red

diffraction-limited spots (N_{foci}) collected from 106 distinct DNA molecules ($N_{DNA\text{-}ORC}$). The dashed lines indicate the location of the NPSs, and the solid curve indicates the kernel density estimation of the data. (ii) Spatial distribution of ORC on DNA containing a chromatinized origin as deduced from the red diffraction-limited spots (N_{foci}) collected from 50 distinct DNA molecules ($N_{DNA\text{-}ORC}$) analysed and displayed as in panel (b-i). (iii) Spatial distribution of ORC on DNA containing a non-chromatinized mutated origin as deduced from the diffraction-limited red spots (N_{foci}) collected from 70 distinct DNA molecules ($N_{DNA\text{-}ORC}$) analysed and displayed as in panel (b-i). (iv) Spatial distribution of ORC on DNA containing a chromatinized mutated origin as deduced from the red diffraction-limited spots (N_{foci}) collected from 51 distinct DNA molecules ($N_{DNA\text{-}ORC}$) analysed and displayed as in panel b-i. **(c)** ORC occupancy probability for the bins containing the (chromatinized or not) origin in panels (b-i)-(b-iv). Error bars are one-sigma Wilson confidence intervals. Statistical significance is determined by a two-sided binomial test: * $p < 0.05$, ****** $p < 0.0000005$.

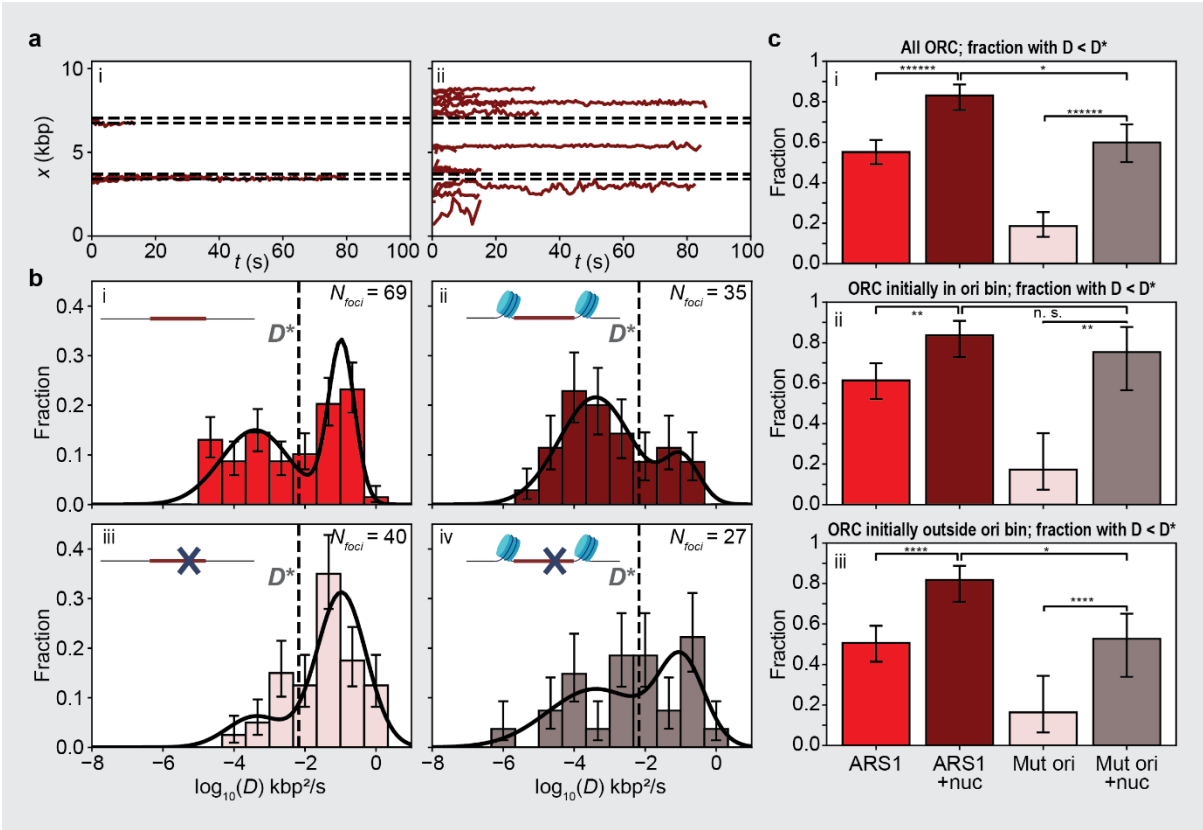

Figure 3. Mobility of ORC on 10.4 kbp DNA containing a chromatinized origin. (a) Traces collected on DNA containing a chromatinized origin illustrating motion of JF646-ORC (i) initially localized within the bin containing the chromatinized origin or (ii) initially localized elsewhere. **(b)** Histograms of the diffusion constants of ORC on DNA molecules containing (i) a non-chromatinized origin, (ii) a chromatinized origin, (iii) a non-chromatinized mutated origin, and (iv) a chromatinized mutated origin. Only foci containing 1 or 2 ORC are included in the analysis (N_{foci}). Error bars are one-sigma Wilson confidence intervals. The observed bimodal distribution is fitted to a double log-normal function (solid black line) which identifies a slowly moving or static ORC subpopulation (55% of the distribution with 0.0049 ± 0.0028 kbp^2/s, mean ± SEM) and a fast diffusive ORC subpopulation (0.152 ± 0.023 kbp^2/s, mean ± SEM). The dashed line indicates the average of the means of the two normal distributions used to fit $\log_{10}(D)$; this average is used as a threshold (D^*). The means of these

subpopulations are imposed in the fits to the data in panels (ii-iv). **(c)** Examination of the slowly moving or static ORC subpopulation. (i) Fitted proportion of the slowly moving or static ORC subpopulation for the datasets in panels (b-i)-(b-iv). (ii) The subpopulation of ORC initially localized within the bin containing the (chromatinized or not) origin was extracted from the dataset; the fraction of this subpopulation that is slowly moving or static ($D < D^*$) is shown here. (iii) The subpopulation of ORC initially localized outside the bin containing the (chromatinized or not) origin was extracted from the dataset; the fraction of this subpopulation that is slowly moving or static ($D < D^*$) is shown here. Error bars are one-sigma Wilson confidence intervals. Statistical significance is determined by a two-sided binomial test: n. s. not significant, * $p < 0.05$, ** $p < 0.005$, **** $p < 0.00005$, ***** $p < 0.000005$ ****** $p < 0.0000005$.

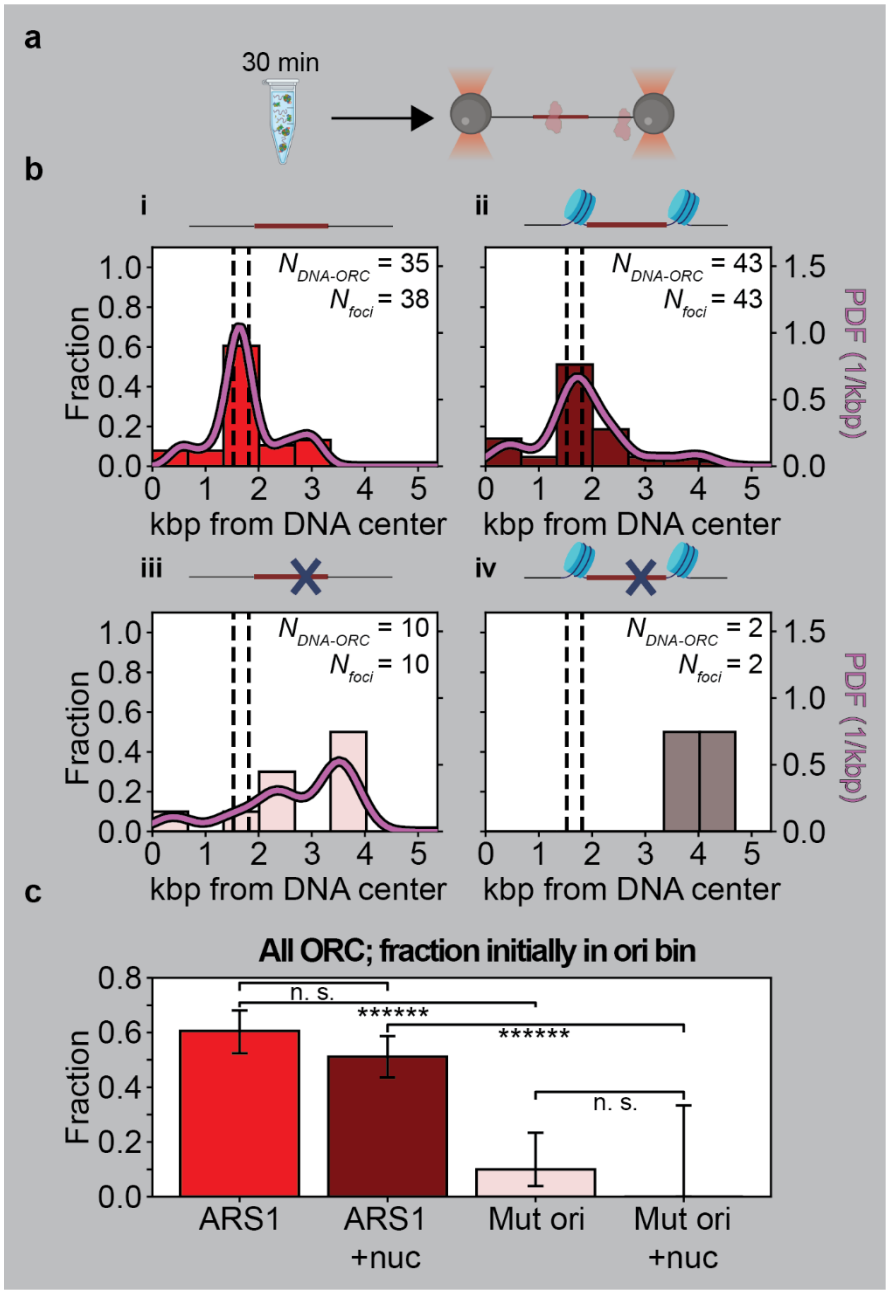

Figure 4. Spatial distribution of stably bound ORC on 10.4 kbp DNA containing a chromatinized origin. (a) Incubation method pertaining to data in panels (b-c). ORC and Cdc6 are incubated with DNA molecules (chromatinized or not, as indicated) in bulk for 30 min in the presence of ATP. Subsequently, the DNA-protein construct is flushed into the single-molecule flow cell, tethered, and moved into the buffer channel for confocal scanning. **(b)** (i) Spatial distribution of ORC on DNA containing a non-chromatinized origin as deduced from

the diffraction-limited red spots (N_{foci}) collected from 35 distinct DNA molecules ($N_{DNA\text{-}ORC}$) analysed and displayed as in panel (b-i). (ii) Spatial distribution of ORC on DNA containing a chromatinized origin as deduced from the diffraction-limited red spots (N_{foci}) collected from 43 distinct DNA molecules ($N_{DNA\text{-}ORC}$) analysed and displayed as in panel (b-i). (iii) Spatial distribution of ORC on DNA containing a non-chromatinized mutated origin as deduced from the diffraction-limited red spots (N_{foci}) collected from 10 distinct DNA molecules ($N_{DNA\text{-}ORC}$) analysed and displayed as in panel (b-i). (iv) Spatial distribution of ORC on DNA containing a chromatinized mutated origin as deduced from the red diffraction-limited spots ($N_{DNA\text{-}ORC}$) collected from 2 distinct DNA molecules ($N_{DNA\text{-}ORC}$) analysed and displayed as in panel (b-i). The dashed lines indicate the location of the NPSs, and the solid curve indicates the kernel density estimation of the data. **(c)** ORC occupancy probability for the bins containing the (chromatinized or not) origin in panels (b-i)-(b-iv). Error bars are one-sigma Wilson confidence intervals. Statistical significance is determined by a two-sided binomial test. n.s. not significant, ****** $p < 0.0000005$.

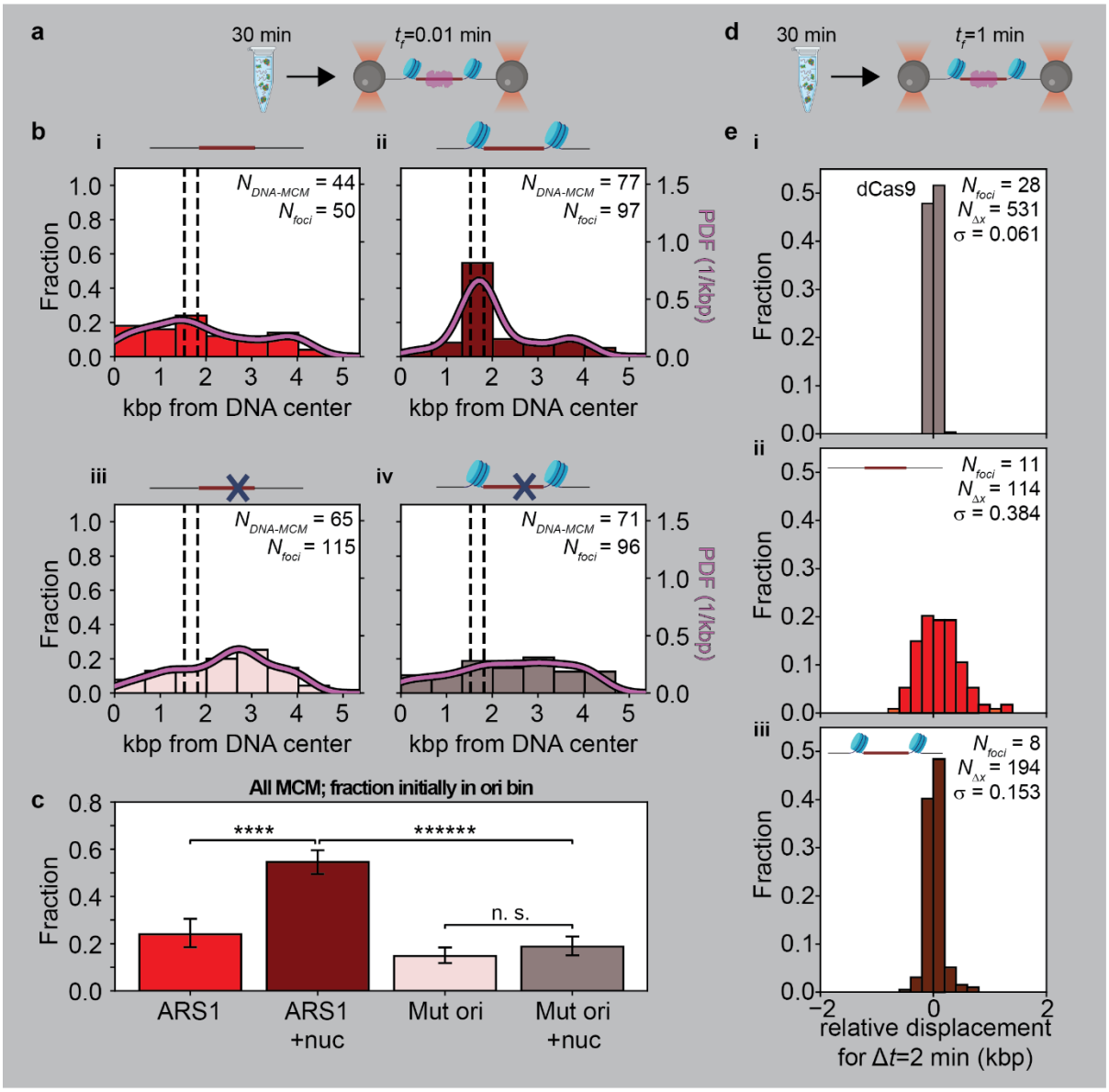

Figure 5. Nucleosomes spatially constrain MCM at the origin. (a) ORC, Cdc6, and Mcm2-7/Cdt-1 are incubated with 10.4 kb DNA molecules (chromatinized or not, as indicated) in bulk for 30 min in the presence of ATP. Subsequently, the DNA-protein construct is flushed into the single-molecule flow cell, tethered and moved into the buffer channel for confocal scanning with an acquisition frequency of one frame every 0.01 min (t_f = 0.01 min). **(b)** (i) Spatial distribution of Mcm2-7 on DNA containing a non-chromatinized origin as deduced from the diffraction-limited red spots (N_{foci}) collected from 44 distinct DNA ($N_{DNA-MCM}$). The dashed lines indicate the location of the NPSs, and the solid curve indicates the kernel density

estimation of the data. (ii) Spatial distribution of Mcm2-7 on DNA containing a chromatinized origin as deduced from the diffraction-limited red spots (N_{foci}) collected from 77 distinct DNA molecules ($N_{DNA\text{-}MCM}$) analysed and displayed as in panel (b-i). (iii) Spatial distribution of Mcm2-7 on DNA containing a non-chromatinized mutated origin as deduced from the diffraction-limited red spots (N_{foci}) collected from 65 distinct DNA molecules ($N_{DNA\text{-}MCM}$) analysed and displayed as in panel (b-i). (iv) Spatial distribution of Mcm2-7 on DNA containing a chromatinized mutated origin as deduced from the diffraction-limited red spots (N_{foci}) collected from 71 distinct DNA molecules ($N_{DNA\text{-}MCM}$) analysed and displayed as in panel (b-i). **(c)** Mcm2-7 occupancy probability for the bins containing the (chromatinized or not) origin for the datasets in panels (b-i)-(b-iv). Error bars are one-sigma Wilson confidence intervals. Statistical significance is determined by a two-sided binomial test: n.s. not significant and ****** $p < 0.0000005$. **(d)** ORC, Cdc6, and Mcm2-7/Cdt-1 are incubated with 10.4 kb chromatinized DNA molecules in bulk for 30 min in the presence of ATP. Subsequently, the DNA-protein construct is flushed into the single-molecule flow cell, tethered and moved into the buffer channel for confocal scanning with an acquisition frequency of one frame per minute (t_f = 1 min). **(e)** Histograms of the relative displacements (Δx = 2 min) between 2 min intervals (Δt = 2 min) for (i) dCas9 molecules over the entire lifetime of the fluorophore for dCas9 molecules, (ii) for Mcm2-7 on DNA containing a non-chromatinized origin or (iii) chromatinized origin. For all three panels, acquisition is continued until the fluorophore is bleached (~20 min). N_{foci}, number of molecules; $N_{\Delta x}$, number of relative displacements; σ, standard deviation.